



Pulmonary and hepatic effects after low dose exposure to nanosilver: Early and long-lasting histological and ultrastructural alterations in rat

E Roda^{a,b}, MG Bottone^b, M Biggiogera^b, G Milanesi^b, T Coccini^{a,*}

^aLaboratory of Clinical & Experimental Toxicology, Toxicology Unit, ICS Maugeri SpA - Benefit Corporation, IRCCS Pavia, via Maugeri 10, 27100, Pavia, Italy

^bLaboratory of Cell Biology and Neurobiology, Department of Biology and Biotechnology "L. Spallanzani", University of Pavia, via Ferrata 9, 27100, Pavia, Italy

ARTICLE INFO

Keywords:

Occupational & environmental exposure
Nanoparticles
Translocation
In vivo toxicity
Risk assessment
Health safety

ABSTRACT

Although environmental airborne silver nanoparticles (AgNPs) levels in occupational and environmental settings are harmful to humans, the precise toxic effects at the portal entry of exposure and after translocation to distant organs are still to be deeply clarified.

To this aim, the present study assessed histopathological and ultrastructural alterations (by means of H&E and TEM, respectively) in rat lung and liver, 7 and 28 days after a single intratracheal instillation (i.t) of a low AgNP dose (50 microg/rat), compared to those induced by an equivalent dose of ionic silver (7 microg AgNO₃/rat). Lung parenchyma injury was observed acutely after either AgNPs or AgNO₃, with the latter compound causing more pronounced effects. Specifically, alveolar collapse accompanied by inflammatory alterations and parenchymal fibrosis were revealed. These effects lasted until the 28th day, a partial pulmonary structure recovery occurred, nevertheless a persistence of slight inflammatory/fibrotic response and apoptotic phenomena were still detected after AgNPs and AgNO₃, respectively.

Concerning the liver, a diffuse hepatocyte injury was observed, characterized by cytoplasmic damage and dilation of sinusoids, engulfed by degraded material, paralleled by inflammation onset. These effects already detectable at day 7, persisting at the 28th day with some attenuations, were more marked after AgNO₃ compared to AgNPs, with the latter able to induce a ductular reaction.

Altogether the present findings indicate toxic effects induced by AgNPs both at the portal entry (i.e. lung) and distant tissue (i.e. liver), although the overall pulmonary damage were more striking compared to the hepatic outcomes.

1. Introduction

Over the past few decades, with advances in nanotechnology and increasing exploitation of engineered nanoparticles (NPs), noble metals NPs, exhibiting significantly unique physic-chemical and biological properties different from their bulk counterparts, have been subject of substantial research [1–4]. Metallic NPs exhibit size and shape-dependent properties that are of interest for applications ranging from catalysts and sensing to optics, textiles, antibacterial activity and data storage [5–11]. Among these NPs, silver NPs (AgNPs), possessing a broad-spectrum of antibacterial properties, strong permeability and little drug resistance, have become one of the most widely used nanomaterials in antibacterial consumer and medical products, i.e. toothpaste, gynecologic suppository, wound dressing and bandages [12–14]. Detailed information about the existing AgNPs global uses are outlined in recent review papers [15–17].

Inevitably, potential adverse effects associated with exposure to AgNPs are of great concern for both workers at nanosilver-manufacturing workplaces and consumers using nanosilver-containing products [18]. As a matter of fact, NPs exposure, by direct or indirect mechanisms, may elicit translocation phenomena triggering unanticipated distant responses, e.g. overt toxic effects involving distant organs such as lung, heart, liver, kidneys, spleen and thymus [13,19–21]. Nanosilver toxicity is still highly disputed both in literature and regulatory bodies reports. In fact, nonetheless the toxicology of macro-sized silver is well established, an in-depth risk assessment of nanosilver is still scrappy, and the available data often controversial [4,13,14,22–26].

A prominent characteristic of AgNP is that it could enhance the organ enrichment of ions, which also allows its extensive application in targeted cancer treatments and biomedical technology [27], nonetheless taking a long period of clearance, possibly triggering toxicity

* Corresponding author.

E-mail address: teresa.coccini@icsmaugeri.it (T. Coccini).

<https://doi.org/10.1016/j.toxrep.2019.09.008>

Received 2 July 2019; Received in revised form 17 September 2019; Accepted 20 September 2019

Available online 22 September 2019

2214-7500/ © 2019 The Authors. Published by Elsevier B.V. This is an open access article under the CC BY-NC-ND license (<http://creativecommons.org/licenses/by-nc-nd/4.0/>).

due to persistence [28,29].

Recent review papers suggest that at the current level of exposure AgNP may not be hazardous to humans and may result in low internal exposure [4,30–32]. Contrarily, accumulating evidences showed AgNP-induced toxicological effects in aquatic ecosystem, causing lethal damage to aquatic plants, aquatic microbes and aquatic vertebrates [33], as well as bacteria and non-mammalian animal species [17,34]. In addition, several investigations using *in vitro* models, further demonstrated size-, dose- and cell-dependent nanosilver cytotoxicity and genotoxicity, including chromosomal abnormalities and inhibition of mitotic processes [17,35–39].

A bulk of literature reports have indicated the oxidative stress as a mechanism playing an important role in cytotoxic effects of AgNPs, able to induce free radicals and reactive oxygen species (ROS) generation and lipid peroxidation, with consequent proteins carbonylation (PCO) [31,35,37,40–43]. In particular, AgNP-induced oxidative stress has been widely demonstrated by recent *in vitro* studies. Onodera and colleagues [44] reported short-term changes in intracellular ROS localization after nanosilver exposure in whole cells and mitochondria in a size-dependent manner. Accordingly, Rajanahalli et al. [45] demonstrated AgNP-triggered ROS production with alteration of the physiological redox-regulated function, leading to gene expression changes and protein modification. Relevantly, another investigation exploring the influence of nanosilver on osteoclastogenesis of human peripheral blood mononuclear cells, revealed an increase in oxidative stress, paralleled by AgNP cellular uptake and endo-lysosomal accumulation [46].

Moreover, a number of *in vivo* experimental investigations revealed that AgNP, in a wide range of concentrations and sizes, were able to induce toxic responses on numerous target organs/systems with different degree of extent, either after single or repeated administration [34,47–52]. AgNPs have been shown to be extremely toxic in small dimension (less than 20 nm), with faster rates of Ag dissolution, but teratogenic in bigger size and larger doses. Additionally, AgNPs produce various toxicogenic responses [53–55], also triggering organ toxicity and inflammatory responses after repeated oral administration *in vivo* [56]. However, despite different exposure routes and animal species have been tested, to deeply comprehend AgNPs kinetics, tissue distribution and overall toxicity [17], the toxicological data coming from *in vivo* studies are still contentious and need to be cautiously interpreted since high unrealistic doses have been often employed.

In the present investigation, with the aim at gaining a broad comprehensive assessment of potential toxic effects on target organs *i.e.* lung and liver, caused by exposure to a commercial nanosilver product, we employed an integrated experimental strategy, comprising *in vivo* toxicology studies as well as AgNPs physicochemical characterization. We focused on specific endpoints and pathological outcomes related to rat pulmonary and hepatic responses after intratracheal instillation (*i.t.*) of a low AgNPs dose (50 µg/rat). Specifically, histochemical and molecular endpoints, in terms of histopathological changes associated to overall toxic response and oxidative stress (*i.e.* tissue/organ and plasma PCO), were investigated. Ultrastructural examination using transmission electron microscopy (TEM) was also performed.

The effects of AgNPs were assessed 7 and 28 days after exposure compared to those caused by administration of an equivalent dose of ionic silver in the form of silver nitrate (7 µg AgNO₃/rat).

2. Materials and methods

2.1. Chemicals

Haematoxylin & Eosin alcoholic solutions were obtained from Ettore Pasquali S.r.L. (Milan, Italy). Antibodies, conjugate and all other chemicals for PCO analyses were purchased from Sigma-Aldrich (Milan, Italy) and Molecular Probes (Eugene, OR, USA). ECL Plus Western blotting detection reagents were obtained from GE Healthcare (Milan, Italy). All chemicals of analytical grade were kindly provided by Eureka

Lab Division (Chiaravalle, AN, Italy).

2.2. Physicochemical characterization of nanoparticles

A 1% water suspension of AgNPs (series PARNASOS® NAMA 39 1103 F01 1%) was kindly provided by Colorobbia S.p.A. (Vinci, Italy).

Before *in vivo* administration, exhaustive physicochemical characterization of AgNPs was performed by scanning transmission electron microscopy (STEM) technique with energy dispersion X-ray (EDX), X-ray powder (XRD) diffraction to determine shape, size distribution, morphology and crystal structure. Specifically, AgNPs were imaged by STEM and energy dispersive x-ray spectroscopy (EDX) was used for point and line profile analysis. EDX was used to determine phase composition of the AgNPs. STEM with high-angle annular dark-field (HAADF) imaging (CAMCOR, University of Oregon, Eugene, OR, USA) was used to determine elemental composition, shape, size distribution, and morphology of nanoparticles.

High-Resolution TEM (HRTEM) operating in Selected Area Electron Diffraction (SAED) mode was applied to obtain information, at small scales, on individual atoms of AgNPs and its defects.

2.3. Animals and experimental design of silver exposure

Thirty-six, 12 weeks old-male Sprague–Dawley rats (Charles River Italia, Calco, Italy), were allowed to acclimatize for at least 2 weeks before treatment, and kept in an artificial 12 h light: 12 h dark cycle with humidity at 50 ± 10% throughout the experiment. Animals were provided rat chow (VRF1 Mucedola diet) and tap water *ad libitum*.

The rat weight was 255 ± 9 g at day of instillation (the time point 0). Groups (n = 6 total, for each treatment group at each time point) of rats were treated with a single intratracheal (*i.t.*) instillation of AgNPs (50 µg/rat). Separate groups of animals received by *i.t.* an equivalent dose of ionic silver in the form of AgNO₃ (7 µg/rat, corresponding to 4.4 µg Ag, as a source for soluble silver ions) or 0.1 ml saline/rat (as control). Before *i.t.* instillation, rats were anesthetized with pentobarbital sodium.

The different applied doses (AgNPs and AgNO₃), duration and route of exposure were chosen accordingly to previous investigations demonstrating that (i) a single 50 µg AgNPs/rat *i.t.* administered triggered pulmonary toxicity and NPs translocation to different target organs [57], and (ii) the Ag fraction present in ionic form in a Silver NPs suspension (14 ± 4 nm in diameter) was about 11% of the total Ag concentration, remaining this fraction stable for several months in suspension [23,58]. Thus, supposing that the AgNPs used in the present study released 11% of their Ag content as ionic silver, it is expected that the animals treated with 50 µg/rat of AgNPs received approximately 6 µg/rat of silver ions.

Regarding *i.t.* instillation, it is a more artificial route of dosing bolus material to the lungs and differences exist in distribution, behaviour, clearance and retention of materials when administered by *i.t.* compared to inhalation; nonetheless, *i.t.* instillation is widely used to address specific endpoints regarding the toxicity of nanomaterials [57,59–61].

AgNPs suspension was vortexed on ice just before the exposure to force nanoparticle dispersion, avoiding agglomerate formation. No surfactants or solvents were used.

Seven and 28 days after treatment, rats (n = 6 for each treatment group) were euthanized with an overdose *i.p.* injection of 35% chloral hydrate (100 ml/100 g body weight (b.w.)). Blood was withdrawal and centrifuge to obtain plasma and lungs and livers were excised.

In detail, lung preparation for morphohistological evaluations was done by vascular perfusion of fixative. Briefly, the trachea was cannulated, and laparotomy was performed. The pulmonary artery was cannulated *via* the ventricle, and an outflow cannula was inserted into the left atrium. In quick succession, the tracheal cannula was connected to about 7 cm H₂O pressure source to inflate the lungs with air, and

clearing solution (saline with 100 U/ml heparin, 350 mosM sucrose) was perfused via the pulmonary artery. After blood was cleared from the lungs, the perfusate was switched to fixative consisting of 4%paraformaldehyde in 0.1 M phosphate buffer (pH 7.4). After fixation, the lungs were carefully removed (see paragraph 2.5.1).

All tissue samples were processed for histopathology (H & E staining), and ultrastructural evaluation by Transmission Electron microscopy (TEM) and plasma were used for oxidative stress evaluation by PCO determination.

All experimental procedures were performed in compliance with the European Council Directive 2010/63/EU on the care and use of laboratory animals. All animals used in this research have been treated humanely according to the institutional guidelines, with due consideration for the alleviation of distress and discomfort.

2.4. Toxicity signs and body weight measurement

Before and after AgNPs dosing, toxicity signs in rats were carefully observed, including appearance, activities, hair, possible trauma, and potential death. Weight change, as important toxicity index, was measured before i.t. instillation and sacrifice.

2.5. Tissue sampling, histology and ultrastructural morphology evaluations

Lung and liver tissues from all rats ($n = 6$) for each treatment, at each time point (7 and 28 days after i.t. instillation), were processed for the following morphological evaluations.

2.5.1. Rat lung and liver specimens preparation

At necropsy, the top and the bottom regions of the right lungs of control and differently treated animals were dissected. Tissue samples were obtained according to a stratified random sampling scheme which is a suggested method for lung tissue in order to compensate for regional differences, which are known to exist in the lung [62] and to reduce the variability of the sampling means. Simultaneously, the right lateral liver lobes from controls and treated rats were excised and collected.

From each slice, 2–3 blocks were systematically derived, washed in NaCl 0.9% and post-fixed by immersion for 7 h in 4% paraformaldehyde in 0.1 M phosphate buffer (pH 7.4), dehydrated through a graded series of ethanol and finally embedded in Paraplast X-TRA. Eight μm thick sections were cut in the transversal plane and collected on silane-coated slides. Subsequently, to overall evaluate structural changes by light microscopy, H & E staining was performed. The slides were then observed and scored with a bright-field Zeiss Axioscop Plus microscope. Specifically, 5 slides (20 sections) per animal ($n = 6$) were analyzed; 5 microscopic fields were examined in each section for each rat per time/condition. The images were recorded with an Olympus Camedia C-5050 digital camera and stored on a PC running Olympus software.

2.5.2. Transmission Electron microscopy (TEM): UA & LC Staining

Lung and liver fragments (small blocks of about 1 mm^3) were fixed for 4 h by immersion in icecold 1.5% glutaraldehyde (Polysciences, Inc., Warrington, PA, USA) buffered with 0.07 M cacodylate buffer (pH 7.4), containing 7% sucrose, followed by post-fixation in OsO_4 (Sigma Chemical Co., St. Louis, MO, USA) in 0.1 M cacodylate buffer (pH 7.4) for 2 h at 4°C , dehydrated in a graded series of ethanol and embedded in Epon 812. For light microscopy pre-examination, semithin section (1 micrometer thick) were stained with 1% borated methylene blue. For electron microscopy, ultrathin sections (about 600 \AA thick) were cut from the blocks, mounted on uncoated 200-mesh-copper grids, and doubly stained with saturated uranyl acetate in 50% acetone and Reynold's lead citrate solution. The specimens were examined with a Zeiss EM 300 electron microscope operating at 80 kV.

2.5.3. Semiquantitative lung and liver lesion analysis

A scoring system was utilized to evaluate the extent of tissue damage using conventional brightfield microscopy according to a semi-quantitative scale ranging from undetectable (-) to striking (+++). Specifically, 20 sections per animals were analyzed, examining 5 microscopic fields in each section for each rat per time/condition.

The localization and degree of lesions was recorded and graded as follows: (-) absent/undetectable lesions, (+) mild injury, (++) moderate damage, (+++) severe insult, (++++) striking alterations. Specifically, the following alterations were recorded: (i) alveolar structure alteration, inflammatory cells incidence, collagen fibers deposition, apoptotic phenomena and (ii) hepatocytes alteration, sinusoids dilation, inflammatory cells incidence, collagen fibers deposition, basal membrane activation (*i.e.* microvilli increase), steatosis, for lung and liver, respectively.

2.6. Oxidative stress evaluation by detection of protein carbonylation (PCO) in lung, liver and plasma

Lung and liver slices from control, AgNO_3 and NPs-treated rats (7 and 28 days) were homogenized in ice-cold lysis buffer (50 mM Tris-HCl, pH 7.4, 150 mM NaCl, 5 mM EDTA, 1% Triton X-100 supplemented with proteases inhibitors) and plasma samples were diluted in 50 mM PBS, pH 7.4. Both tissue lysates and plasma were quantified for protein content and stored at -80°C until PCO analyses. Briefly, lung (10 μg), liver (10 μg) and plasma proteins (5 μg) were processed for protein carbonylation determination, after derivatization, with anti-DNP antibodies by Western blot immunoassay. Immunostained protein bands were then visualized with enhanced chemiluminescence detection, and protein bands on PVDF membranes were stained with amido black [63–65].

2.7. Statistical analysis

Different lung and liver lesions degree data were not normally distributed; therefore, the non-parametric Kruskal Wallis test was used, followed by Dunn's post hoc test. Statistical significance is indicated with a * (p value < 0.05).

3. Results

3.1. Physicochemical characteristics of silver nanoparticles (AgNPs)

Fig. 1 summarizes the characteristics of the AgNPs.

The brown-colored AgNPs suspension (1% in water) possessed the following characteristics: 1 g/cm^3 density, 3 mPa/sec viscosity (25°C), < 0.50 PDI (polydispersity index) 6.5 pH, and 20 nm nominal hydrodynamic size diameter (supplier data).

Additional analyses were conducted to better characterize the physicochemical properties of the tested AgNPs. Quantitative scanning transmission electron microscopy (STEM) with high-angle annular dark-field (HAADF) imaging showed that NPs contained pure silver, as also indicated by the energy dispersive x-ray (EDX) spectrum (Fig. 1, Panel A and B), being a 25 nm-thick the predominant entity present in the suspension, with a relatively narrow size distribution and no evidence of aggregation (Figs. 1, Panel B). There were no peaks of impurities, being the other minor elements detected related to water background. At atomic scale, High-Resolution Transmission Electron Microscopy (HRTEM) revealed well-dispersed, spherical-shaped AgNPs with a smooth surface, also indicating the presence of two populations of NPs, their size being 10–20 nm (the predominant entity) and 40–50 nm, respectively (Fig. 1, panel C).

The presence of approximately 20 nm pure AgNPs was also confirmed by selected area (electron) diffraction (SAED) pattern analysis (Fig. 1, panel D).

The zeta potential was -15 indicating nanoparticles dispersed in

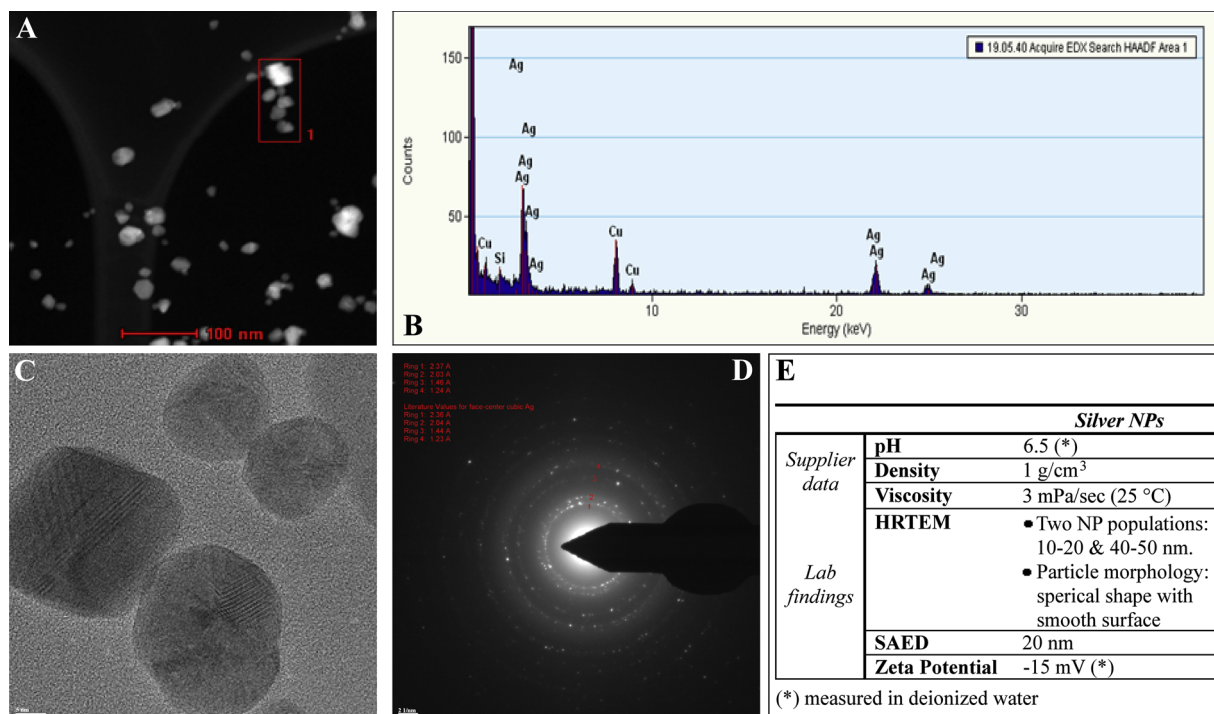


Fig. 1. STEM, HRTEM, SAED images (Panel A–D) and summarized physicochemical properties of AgNPs (Panel E). STEM analysis, including high-angle annular dark-field scanning transmission electron microscopy (HAADF STEM), showed no tendency to aggregate of AgNPs (Panel A). The energy dispersive X-ray spectrum (EDS) analysis, performed on the AgNPs, indicated that the main composition of sample is Ag (Panel B). EDS was used for point and line profile analyses indicated as [1] in STEM image showing AgNP (bar = 100 nm) (Panel A). HRTEM image give information at atomic scale (bar = 5 nm) (Panel C). SAED pattern indicates pure AgNP: four diffraction rings and each coincides with a diffraction ring of pure Ag (bar = 21 nm) (Panel D).

water would remain stable during storage (Fig. 1, panel E). Although there was no tendency to agglomerate, the particle sample was vortexed prior to measurements. For an exhaustive physicochemical characterization, see also Coccini et al. [66].

3.2. Toxicity signs and body weight measurement

No toxicity signs or mortality were observed in rats exposed to both AgNPs or AgNO₃, neither 7 days post treatment nor during the recovery periods (until 28 days). The b.w. gain of control and treated rats were comparable: the b.w. increased by about 40% in all groups from day 0 to the last day of treatment (day 28).

3.3. Histological and ultrastructural data

3.3.1. Lung

After i.t. exposure to the different compounds, namely AgNPs and AgNO₃, the lung parenchyma, analysed by both light and electron microscopy, showed patterns of injury with different extent of intensity, already observable 7 days after i.t. instillation with either AgNPs or AgNO₃, with the latter compound causing stronger effects (Table 1, Fig. 2). Specifically, an alteration of the physiological pulmonary structure was detected, characterized by collapsed alveoli, inflammatory alterations (i.e. enhanced presence of activated macrophages, lymphocytes and other inflammatory cells), thickening of alveolar septa, haemorrhages and parenchymal fibrosis, i.e. collagen overproduction and accumulation. Noticeably, type II pneumocytes were characterized by piles of vacuolized and surfactant-lamellated bodies of various shapes and sizes. Some bronchus-associated prominent lymphoid nodules were evidenced in the peribronchiolar areas by H&E (Fig. 2).

The overall effects observed acutely (7 days after i.t. instillation) lasted until the 28th day, although, during this period, an attenuation of the toxic signs occurred (Table 1 and Fig. 3). In particular, at this later

timepoint, a partial recovery of the pulmonary structure was detected after both compounds (Table 1), nonetheless still accompanied by AgNPs-caused inflammatory response and parenchymal fibrosis, i.e. diffuse encapsulated collagen fibres deposition (Figs. 3 and 4), and AgNO₃-induced apoptotic phenomena (Fig. 3).

3.3.2. Liver

The histological and ultrastructural evaluation of the liver demonstrated a tissue damage, with a different degree based on the diverse instilled compound, i.e. AgNPs vs AgNO₃, already detectable at 7 days-post treatment (Table 1 and Figs. 5 and 6), which persisted at the 28th day with some attenuations (Table 1 and Fig. 7). Compared to the overall marked damage observed in lung, the alteration detected in liver was milder.

In detail, after exposure to both compounds, a diffuse hepatocyte injury was observed, characterized by cytoplasmic damage and dilation of sinusoids evidently engulfed by degraded material (Figs. 5 and 6). Early onset of inflammation was also observed, characterized by the increased presence of several inflammatory cells, including several activated Kupffer cells, and phagosomes. Moreover, a fibrotic response was demonstrated by an evident accumulation of collagen fibres, particularly abundant in the space of Disse (Fig. 6). No evident alteration of the centrilobular vein and ducts was observed at both considered timepoints, with exception for an early ductular reaction clearly detected at the 7th day after AgNPs only (Fig. 5).

As a peculiar effects caused by AgNO₃ only, the basal membrane activation, with an evident increase of microvilli in the perisinusoidal space was observed, already at day 7 post-treatment, still persisting at the day 28 (Figs. 6 and 7).

Notably, at the later timepoint after the recovery period (day 28), an attenuation of hepatic injury was perceived, after both AgNPs and AgNO₃, in terms of (i) recovery of the cytoplasmic integrity and (ii) absence of fibrotic response (i.e. lack of collagen fibres accumulation), nonetheless paralleled by both inflammatory phenomena persistence

Table 1
Semi-quantitative scoring of lung and liver lesions in control and treated rats. Degree scale: from absent (–) to striking (++++) followed by Kruskal–Wallis followed by Dunn's post hoc test: (***) < 0.01; (***) < 0.05; ns = not statistically significant.

7 DAYS													
LUNG													
	Controls (n = 6 rats)			AgNPs (n = 6 rats)			AgNO ₃ (n = 6 rats)			(*) Total Average Score			
	#1	#2	#3	#4	#5	#6	#1	#2	#3	#4	#5	#6	
Alveolar structure alteration	–	–	–	–	–	–	+++	+++	+++	+++	+++	+++	+++
Inflammatory cells incidence	–	±	–	–	–	±	+	+	+	+	+	+	+
Collagen fibres deposition	–	–	–	–	–	–	++	++	++	++	++	++	±
Apoptosis	–	–	–	–	–	–	±	±	±	±	±	±	+
(*) TOTAL AVERAGE SCORE													
	Controls			AgNPs			AgNO ₃			p value			
Alveolar structure alteration	–			+++			+++			*			
Inflammatory cells incidence	±			++			++			*			
Collagen fibres deposition	–			++			+			*			
Apoptosis	–			+			+			*			
28 DAYS													
LUNG													
	Controls (n = 6 rats)			AgNPs (n = 6 rats)			AgNO ₃ (n = 6 rats)			(*) Total Average Score			
	#1	#2	#3	#4	#5	#6	#1	#2	#3	#4	#5	#6	

Alveolar structure alteration	–	–	–	–	–	–	++	++	++	++	++	++	++
Inflammatory cells incidence	–	±	–	–	–	–	±	±	±	±	±	±	±
Collagen fibres deposition	–	–	–	–	–	–	++	++	++	++	++	++	±
Apoptosis	–	–	–	–	–	–	+	+	+	+	+	+	+
(*) TOTAL AVERAGE SCORE													
	Controls			AgNPs			AgNO ₃			p value			
Alveolar structure alteration	–			++			++			*			
Inflammatory cells incidence	–			+			+			*			
Collagen fibres deposition	–			++			±			*			
Apoptosis	–			+			+			*			

(continued on next page)

Table 1 (continued)

7 DAYS																
LIVER																
	Controls (n = 6 rats)			AgNPs (n = 6 rats)			AgNO ₃ (n = 6 rats)			AgNO ₃ (n = 6 rats)			Total Average Score (*)	p value		
	#1	#2	#3	#4	#5	#6	Total Average Score (*)	#1	#2	#3	#4	#5			#6	Total Average Score (*)
Hepatocytes alteration	-	-	-	-	-	-	-	++	++	++	++	++	+++	+++	++	
Sinusoids dilation	-	-	-	-	-	-	-	+	+	+	+	+	+	+	++	
Inflammatory cells incidence	-	±	-	±	±	±	±	++	++	++	++	++	+++	+++	++	
Collagen fibres deposition	-	-	-	-	-	-	-	+	+	+	+	+	+	+	+	
Basal membrane activation (i.e. microvilli increase)	-	-	-	-	-	-	-	-	-	-	-	-	±	±	+	
Ductular reaction	-	-	-	-	-	-	-	+	++	++	+	+	±	±	-	
Steatosis	-	-	-	-	-	-	-	-	-	-	-	-	±	±	-	
(*) TOTAL AVERAGE SCORE																
	Controls						AgNPs						AgNO ₃			
Hepatocytes alteration	-	-	-	-	-	-	-	++	++	++	++	++	++	++	+	*
Sinusoids dilation	-	-	-	-	-	-	-	+	+	+	+	+	+	+	+	*
Inflammatory cells incidence	-	±	-	±	±	±	±	++	++	++	++	++	+++	+++	++	*
Collagen fibres deposition	-	-	-	-	-	-	-	+	+	+	+	+	+	+	+	*
Basal membrane activation (i.e. microvilli increase)	-	-	-	-	-	-	-	-	-	-	-	-	±	±	+	*
Ductular reaction	-	-	-	-	-	-	-	++	++	++	+	+	±	±	+	**
Steatosis	-	-	-	-	-	-	-	-	-	-	-	-	-	-	-	ns
28 DAYS																
LIVER																
	Controls (n = 6 rats)			AgNPs (n = 6 rats)			AgNO ₃ (n = 6 rats)			AgNO ₃ (n = 6 rats)			Total Average Score (*)	p value		
	#1	#2	#3	#4	#5	#6	Total Average Score (*)	#1	#2	#3	#4	#5			#6	Total Average Score (*)
Hepatocytes alteration	-	-	-	-	-	-	-	±	+	±	±	±	+	+	+	
Sinusoids dilation	-	-	-	-	-	-	-	+	+	+	+	+	+	+	+	
Inflammatory cells incidence	-	-	±	±	±	±	±	+	+	+	+	+	+	+	+	
Collagen fibres deposition	-	-	-	-	-	-	-	-	-	-	-	-	-	-	-	
Basal membrane activation (i.e. microvilli increase)	-	-	-	-	-	-	-	-	-	-	-	-	-	-	-	
Ductular reaction	-	-	-	-	-	-	-	-	-	-	-	-	-	-	-	
Steatosis	-	-	-	-	-	-	-	+	++	++	++	++	+++	+++	++	
(*) TOTAL AVERAGE SCORE																
	Controls						AgNPs						AgNO ₃			
Hepatocytes alteration	-	-	-	-	-	-	-	+	+	+	+	+	+	+	+	*
Sinusoids dilation	-	-	-	-	-	-	-	++	++	++	++	++	++	++	++	*
Inflammatory cells incidence	-	±	-	±	±	±	±	+	+	+	+	+	+	+	+	*
Collagen fibres deposition	-	-	-	-	-	-	-	-	-	-	-	-	-	-	-	ns
Basal membrane activation (i.e. microvilli increase)	-	-	-	-	-	-	-	-	-	-	-	-	-	-	-	*
Ductular reaction	-	-	-	-	-	-	-	++	++	++	+	+	±	±	+	ns
Steatosis	-	-	-	-	-	-	-	-	-	-	-	-	-	-	-	*

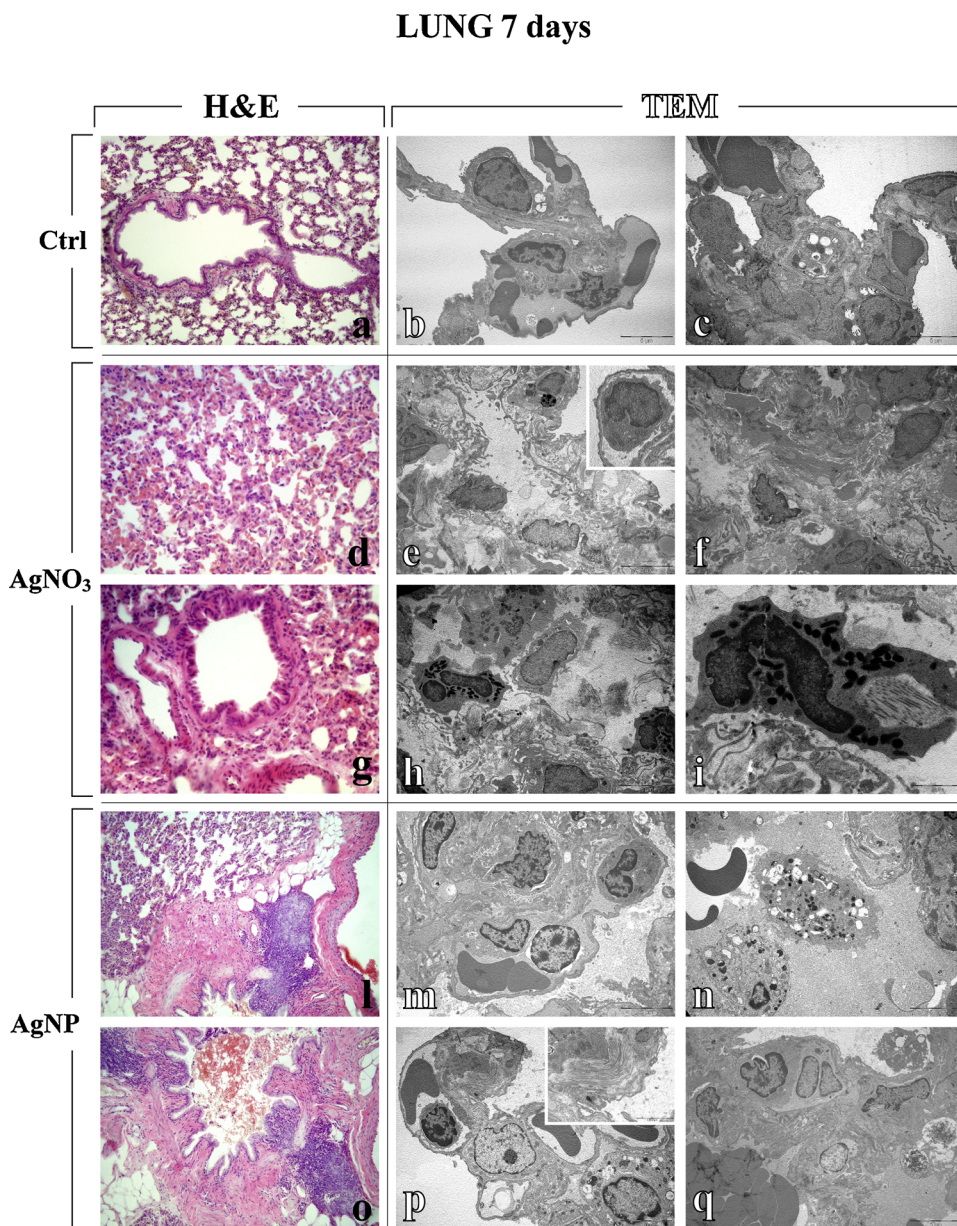


Fig. 2. Representative lung parenchyma specimens, investigated by both Light (H&E) and Electron microscopy - TEM (a, d, g, l, o and b–c, e–f, h–i, m–n, p–q, respectively), from control (a–c), AgNO₃- (d–i) and AgNP-treated (l–q) rats, 7 days after i.t. instillation. The physiological pulmonary structure is clearly preserved in control animals (a–c). Differently, selected structural alterations evidenced in pulmonary parenchyma of both AgNO₃- and AgNPs-treated rats are presented. Collapsed alveoli characterized by wall thickening and micro haemorrhagic foci, along with bronchiolar distortion (d, g and l); bronchus-associated lymphoid nodules adjacent to granulomatous formation in peribronchiolar area (l and o); markedly degraded pulmonary structure, with diffuse presence of collagen fibres (e–f), with detail of activated monocyte (insert in e); damaged lung parenchyma with several activated eosinophil granulocytes (h), characterized by the presence of cytoplasmic phagosomes, collagen fibres and residual bodies (i); thickened alveolar wall stuffed with inflammatory cells (m); early and late apoptosis (n); type II pneumocytes (PII) packed with vacuolized multi-vesicular bodies, activated lymphocyte in a vessel (p), and collagen fibril bundles (insert in p); pulmonary thrombus, together with necrosis (q). *Light microscopy magnification: 20x (a, l, and o); 40 x (d and g). Electron Microscopy original magnification: x 5,000 (b–c, e–f, h, m–n, p–q); x 12,000 (i); x 20,000 (insert in p).*

(Table 1 and Fig. 7). Further, the exclusively AgNO₃-induced basal membrane activation was still observed (Fig. 7).

Unexpectedly, a late (28 days) occurrence of steatosis was observed, ultrastructurally characterized by the widespread presence of fat vacuoles occupying the greater part of the hepatocytes, pushing the nucleus to the periphery (Fig. 7).

3.4. Oxidative Stress Evaluation by PCO Assessment in lung, liver and plasma

At both considered time points (*i.e.*, 7 and 28 days after a single i.t. instillation), treatment with AgNPs or AgNO₃ did not induce any increase in protein carbonyls in both tissue homogenates and plasma proteins, compared to controls (data not shown).

4. Discussion

The present study addresses the pulmonary and hepatic effects resulting from translocation of commercial AgNPs, 7 and 28 days after a single i.t. instillation in rats. The outcomes were compared with those

caused by AgNO₃.

Altogether, our histological and ultrastructural data indicate the occurrence of early- and long-lasting injury in lung and liver of rats after a single AgNPs i.t. low dose administration. The employed bulk AgNO₃ counterpart caused similar adverse effects with a more marked extent, also triggering apoptotic phenomena at the delayed timepoint. Specifically, light microscopy and TEM analyses depicted the onset of evident histopathological changes of the pulmonary and hepatic architecture, mainly accompanied by inflammation and fibrosis, while any sign of PCOs generation was detected.

The adverse effects appeared early (at day 7) and lasted until 28 days post-exposure, with some attenuation of the toxic signs occurring during this recovery period. Notably, the lung was the most damaged organ, being the hepatic alteration less evident. Specifically, based on (i) data presented in Table 1, including whole data (single and total average scores followed by statistical significance analysis) coming from each rat involved in the study, and (ii) TEM and H&E micrographs, more marked alterations of the pulmonary cytoarchitecture, associated with fibrosis occurrence, was clearly observable compared to those detected for hepatic tissues.

LUNG 28 days

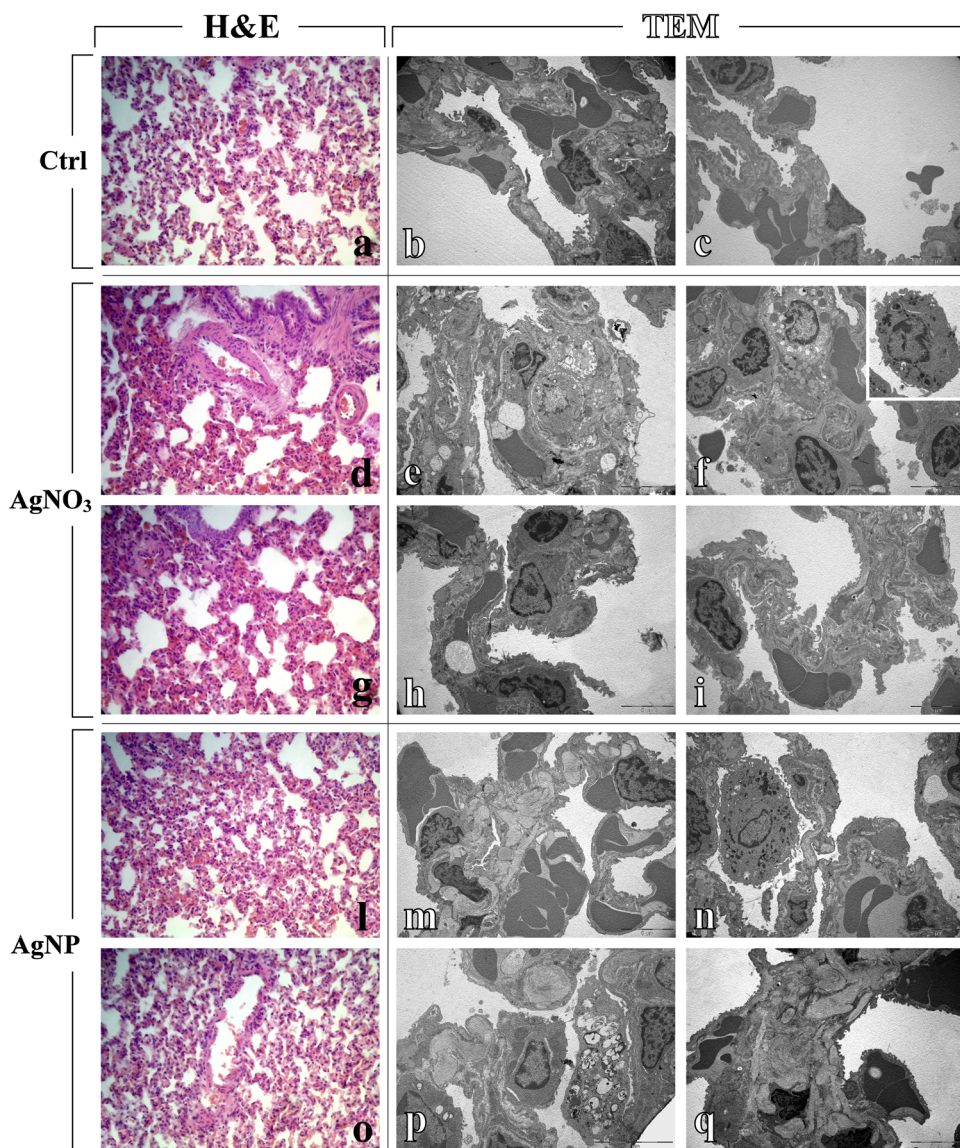


Fig. 3. Light (H&E) and electron microscopy (TEM) micrographs (a, d, g, l, o and b–c, e–f, h–i, m–n, p–q, respectively), showing lung tissue of control (a–c), AgNO₃- (d–i) and AgNPs-treated (l–q) rats, 28 days after i.t. instillation. Normal alveolar and bronchiolar morphology is visibly conserved in controls (a–c), while morphological and ultrastructural alterations are manifest in the lungs of treated animals, after both AgNO₃ and AgNPs. Collapsed alveoli, associated with architectural distorted bronchioli, both exhibiting wall thickening (d, g, l and o); markedly damaged alveolar area showing apoptotic and necrotic cell death (e); altered, thickened alveolar wall, characterized by the presence of type II pneumocytes (PII) filled by vacuolized multi-vesicular bodies (f), with detail of activated monocyte (insert in f); early apoptosis (h); injured alveolar wall displaying limited presence of collagen fibres (i); haemorrhagic blood clots close to collagen engulfed areas (m and q); activated macrophage and apoptosis (n); type II pneumocytes (PII) filled by vacuolized multi-vesicular bodies together with extensive deposition of encapsulated collagen fibril bundles (p). *Light microscopy magnification: 40x (a, d, g, l and o). Electron Microscopy original magnification: x 5,000 (b–c, e–f, h–i, m–n, q); x 7,500 (p).*

LUNG 28 days

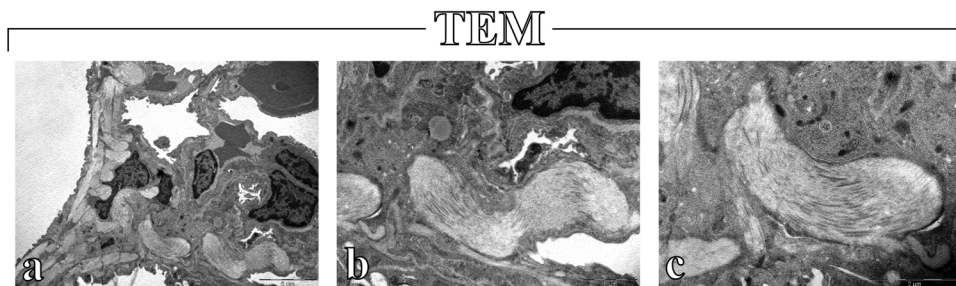


Fig. 4. Electron microscopy images showing the widespread deposition of abundant encapsulated collagen fibril bundles in the alveolar and stromal areas 28 days after i.t exposure to AgNPs (a–c). *Original magnification: x 5,000 (a), x 12,000 (b) and x 20,000 (c).*

Interestingly, at the early timepoint (7 days post-exposure), AgNPs treatment induced either a pronounced inflammation, i.e. enhanced presence of activated macrophages and Kupffer cells, as well as a strong

fibrotic reaction, as evidenced by the presence of widespread encapsulate collagen fibres deposition, both in lung parenchyma as well as in liver, with the effect lasting until 28 days in lung only.

LIVER 7 days

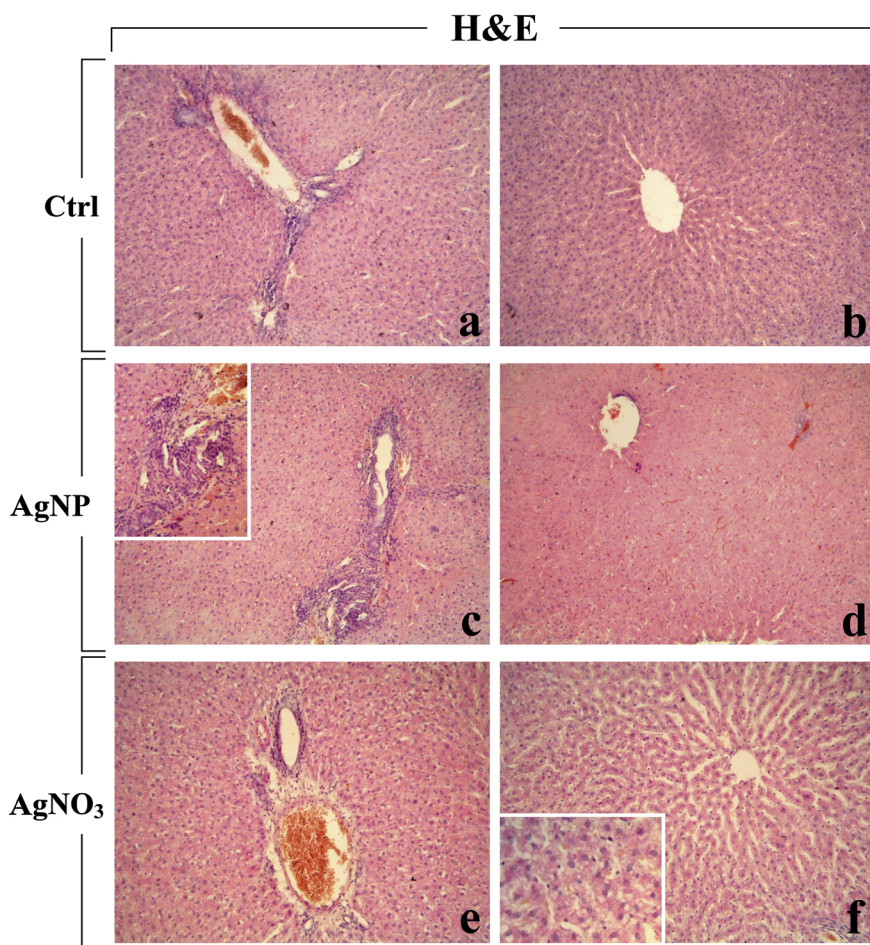


Fig. 5. Representative H&E-stained liver specimens from control animals (a–b) and rats exposed to AgNPs (c–d) and AgNO₃ (e–f), 7 days post-instillation. The physiological hepatic structure is clearly well preserved in control rats (a–b). No striking alteration of the centrolobular vein, ducts and portal area was observed after AgNO₃, even though accompanied by a hepatocyte alterations, i.e. cytoplasmic damage and dilation of sinusoids (e–f). In AgNP-treated rats, an early ductular reaction was clearly visible (c), while no marked alteration of the portal area was observed (d). Objective magnification: 20x (a–b, c–d, e–f); 40x (insert in c), 60x (insert n f).

Notably, early post-exposure (day 7), the AgNPs-induced occurrence of fibrosis in liver was accompanied by a ductular reaction. This result is in line with previous experimental findings both in humans and animal models, demonstrating a strong causal relationship between the extent of ductular reaction and fibrosis across a range of liver injury, even though which mechanism is the primary one still remained an unresolved question [67]. Hence, the observed ductular reaction may be an alternative regenerative pathway, which compensate for the advancement of fibrosis and the transient impairment of the hepatocytes regenerative activity, possibly contributing to a recovery process, leading to a complete recovery of the fibrotic phenomena observed 28 days-post-treatment in liver.

Regarding to the oxidative stress pathway, evaluated by PCOs determination, our data clearly indicated that after a single i.t. exposure to either AgNPs or AgNO₃, the PCOs occurrence was similar to that observed in control rats, thus demonstrating the complete lack of oxidative stress effects in both lung and liver as well as in plasma samples, at both considered time points (i.e., 7 and 28 days after treatment).

Published literature reports indicate that the unquestionable AgNPs peculiar properties/advantages are nonetheless paralleled by serious hazard to various organisms [1,17,48,68], in a wide range of concentrations and sizes, being the smaller the most hazardous. As a matter of fact, AgNPs accumulate in target organs of animals through several administration routes, thereby inducing toxic effects such as cell dysfunction, inflammation, DNA damage and, sometimes, animal death [17,34,55,69–71].

Moreover it has to be taken into consideration that environmental

airborne AgNPs levels (5–289 mg/m³) in occupational and environmental settings are harmful to human lungs due to inhalation of NPs. Thus, i.t. studies in animals, using appropriate dosage simulating these mentioned exposure conditions, may provide relevant information for assessing toxicity arising from airborne NPs [17,72–74].

Therefore, with the goal to study the toxic effects of AgNPs at low-level, which may mirror occupational, environmental and also consumer exposure scenario [26,57,75], in the present investigation, an i.t. dose of 50 microg AgNPs/rat (corresponding to a dose of about 200 microg/kg b.w.) was tested. This concentration was chosen based on previous investigations by Takenaka et al. [57], employing AgNPs (15 nm modal diameter) administered by two different treatment routes, namely i.t. instillation or inhalation. The authors reported (i) lung toxicity and NP translocation, leading to deposition in distant organs, after i.t. exposure (50 microg AgNPs/rat); (ii) differential Ag accumulation after inhalation protocol (correspondent dose of 133 microg/m³ AgNPs, for 6 h-exposure), with the highest concentration measured in lungs and blood, while the lowest found in liver, kidneys, spleen, brain and heart. In detail, inductively coupled plasma mass spectrometry (ICP-MS) analysis, performed after instillation study, demonstrated that (i) only 9–16 microg of the total instilled 50 microg AgNP was retained in the lung one day after i.t. exposure, persisting unchanged until day 7, while (ii) Ag content in the liver was $113 \pm 24 \text{ ng} \times \text{organ weight}$ one day after treatment, decreasing to about 29 ± 10 and $16 \pm 7 \text{ ng} \times \text{organ weight}$ at day 4 and 7, respectively.

Furthermore, a recent *in vivo* investigation testing AgNPs (100

LIVER 7 days

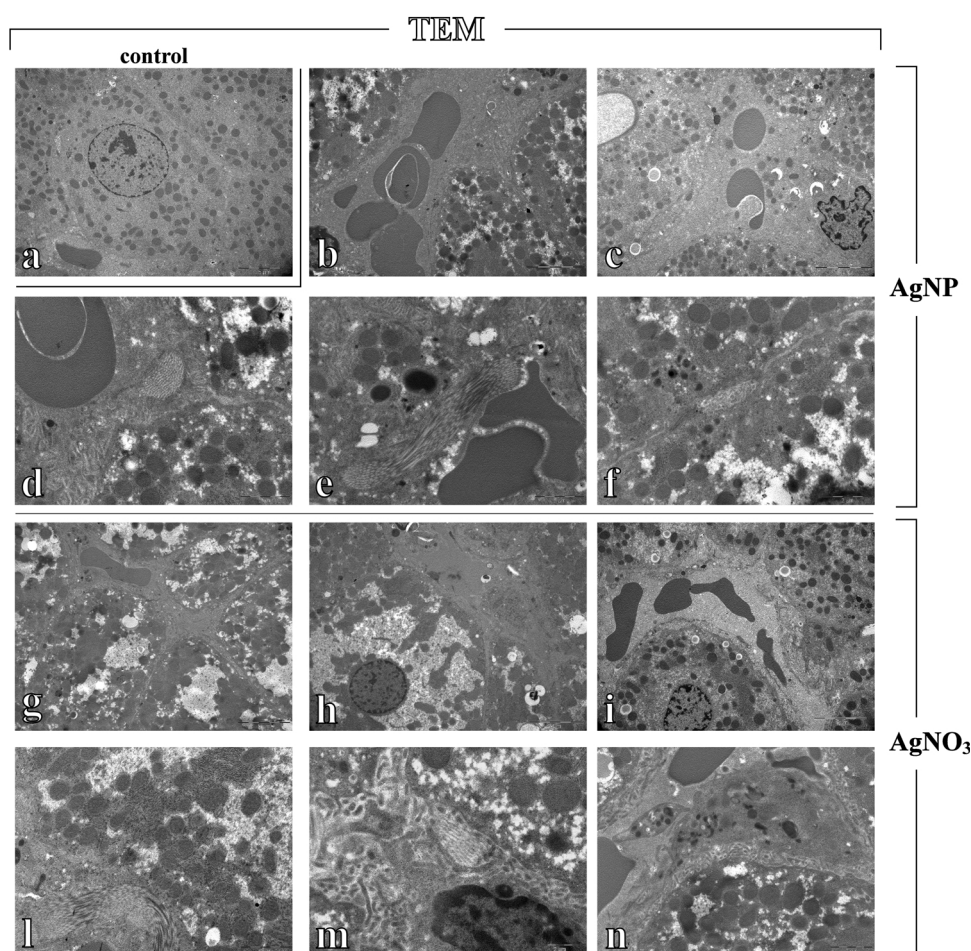


Fig. 6. TEM micrographs illustrating liver tissue of control (a), AgNPs (b–f) and AgNO₃-treated (g–n) rats, 7 days after i.t. instillation. Normal hepatic morphology is manifestly preserved in controls (a), whereas ultrastructural changes are observable in the liver of treated animals, after both AgNO₃ and AgNPs. Haemorrhagic blood clots in enlarged sinusoid together with inflammatory cells, close to damaged cytoplasmic areas (b); dilated sinusoid engulfed with cellular debris (c); enlarged hepatic sinusoid showing an increase of characteristic microvilli (d); increased collagen fibers in perisinusoidal space of Disse (e); dilated biliary canaliculus in a degraded cytoplasmic region (f). Widespread ultrastructural damage with dilated sinusoid engulfed with cellular debris (g and h), often accompanied by increased microvilli (i); collagen fibres deposition (l); space of Disse with inflammatory cells (m); hepatocyte showing damaged cytoplasm, close to enlarged sinusoid characterized by the presence of Kupffer cells and cellular degraded material (n). Original magnification: $\times 5,000$ (a–c, h–i); $\times 12,000$ (d–g, l); $\times 20,000$ (m); $\times 10,000$ (n).

microg/mouse) administered by repeated oropharyngeal aspiration, demonstrated marked toxic effects in lung, paralleled by NP translocation to secondary organs, examined 2 and 28 days after final treatment. Elemental analysis (ICP-MS), paralleled by histopathological data, demonstrated (i) an evident increase of Ag in the lungs at both time points, most pronounced at day 2 (Ag content about 100 ng/mg tissue), still elevated at day 28 (about 20 ng/mg tissue); (ii) a liver Ag content about 0.03 ng/mg tissue at the first evaluated timepoint, decreasing about three-fold at the latest detection [76].

Undeniably, these above reported findings demonstrated that, other than lung, liver is one of the main target organs of AgNPs, as a consequence of the ability of NPs to reach secondary organs *via* the blood circulation system. A bulk of experimental studies, using different exposure routes involving translocation of NPs, demonstrated a time- and size-dependent accumulation of AgNPs in liver causing a severe negative effects ranging from pathological changes of tissue cytoarchitecture to enzymatic activity alteration, possibly leading to liver dysfunction and eventual apoptosis [31,69,70,77–79]. On the other hand, a recent *in vitro* and *in vivo* investigation demonstrated that biologically synthesized AgNP, functionalized using *M. alba* leaf extract, possessed hepatoprotective activity, supporting their use as a novel drug able to treat hepatocellular diseases [80].

It has to be mentioned that the most part of these available *in vivo* studies, revealing AgNPs tissue distribution and overall toxicity, employed high and unrealistic doses, administered using non-physiological exposure routes. Notably, in the attempt to overcome this limitation, the effects of a low AgNPs dose (10 microg Ag/mouse; i.t.

administration) has been recently investigated, reporting either lung toxicity, in terms of inflammatory pathway activation, as well as AgNPs translocation to distant organs [61]. In particular, pulmonary Ag concentration measured 4 and 24 h after instillation, was significantly higher in AgNP-treated mice, compared to animal receiving the same dose of AgNO₃. Notably, already 4 h after instillation, only a trace amount of Ag was detected in the liver of AgNPs-treated mice (about 0.041 ± 0.033 microg/g tissue), while, differently, 7% of the initial Ag dose was measured in the liver of animals exposed to AgNO₃. Arai and colleagues suggested that Ag ionic form would be readily absorbed by the lung tissue, entering the systemic circulation more efficiently than AgNPs. Remarkably, at the later timepoint (24 h after exposure) the Ag concentration in the liver was undetectable, being below Limit of detection (LOD).

Another work by Silva et al. [75] investigating AgNPs concentration approximating human occupational and consumer exposure in a worst-case scenario, explored the toxic effects of AgNPs (nominal diameters 20 and 110 nm) administered by a single i.t. exposure at low doses (30–300 microg/rat). Peculiarly, significant inflammation throughout the experimental time course (1–21 days) was induced by the highest doses only, characterized by pathological alterations of lung parenchyma. A recent experimental *in vivo* investigation, testing either a single AgNP low-dose i.t. instilled or repeated non-lethal single doses intraperitoneally injected, supported the use of several bioprotective complexes (including pectin, some vitamins, glutamate, glycine, N-acetylcysteine, omega-3 PUFA) to improve organism's resistance to nanosilver-caused adverse effects, as a valuable auxiliary tool in

LIVER 28 days

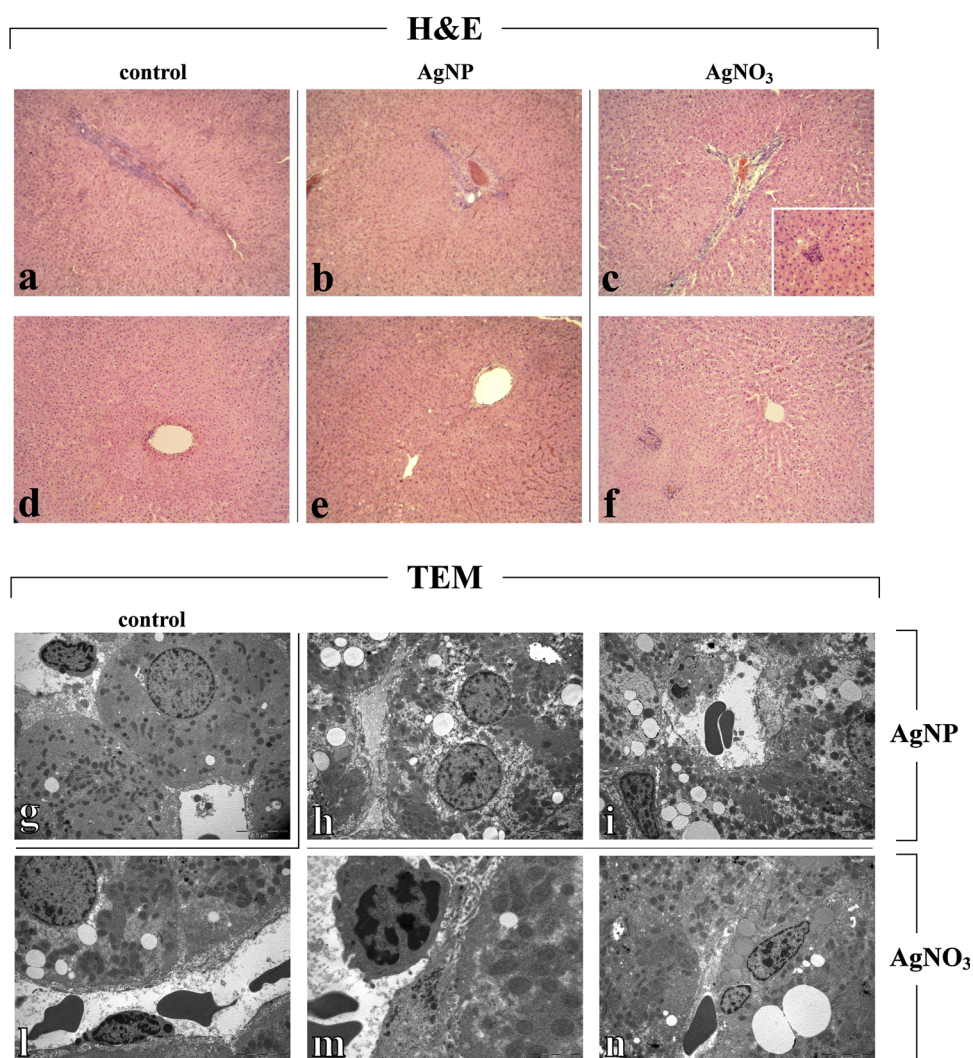


Fig. 7. Representative liver specimens, investigated by both Light (H&E) and Electron microscopy - TEM (a–f and g–n, respectively), from control (a,d and g), AgNP- (b, e, h–i) and AgNO₃-treated (c, f, l–n) rats, 28 days after i.t. instillation. The normal hepatic structure is conserved in control animals (a, d and g). H&E micrographs show an attenuation of hepatic injury, after both AgNPs (b and e) and AgNO₃ (c and f). No evident changes in centrilobular vein, ducts and portal area are shown, nonetheless the presence of inflammatory cells clusters are still observable in AgNO₃-treated rats only (c). TEM images show in detail ultrastructural alterations in liver of both AgNO₃- and AgNPs-treated rats. Hepatocytes displaying slightly damaged cytoplasm, characterized by the presence of several fat vacuoles (h and n), close to Ito cell (i). Hepatocyte with quite homogeneous cytoplasm, scarcely damaged, close to enlarged sinusoid showing basal membrane activation, i.e. increased microvilli, and evident endothelial cells (l); activated monocyte in the sinusoidal lumen (m). *Light microscopy magnification: 20x (a–f), 40x (insert in c). Electron Microscopy original magnification: x 5,000 (g, h–i, l, n) x 12,000 (m).*

occupational health risk management [81].

In the present study, we employed a low AgNPs dose (50 microg/rat corresponding to 200 microg/kg b.w.) compared to an equivalent dose of ionic silver in the form of AgNO₃. The selected AgNP dose and type were chosen to mimic occupational and consumer exposure to engineered NPs (ENPs) often employed in paints, coatings and pigment industry [61,76,82]. Occupational exposure to AgNPs used in this field can occur during the production, handling and application processes, while consumer activities such as scratching (by children and pets), cleaning and UV exposure can damage the coatings leading to NPs release into the environment. Therefore, respiratory inhalation of environmental dust allow NPs to enter the body through the pulmonary system or skin, reaching the bloodstream, and then being transported to secondary target organs [83–85].

Accordingly, our data using a low realistic dose introduced by pulmonary instillation, highlighted a marked AgNPs-induced lung toxicity, paralleled by the clear involvement of a secondary organ i.e., the liver, even though the detected hepatic alterations were milder. We demonstrated that AgNPs-caused adverse effects appeared already 7 days after exposure and lasted until day 28, with attenuation of the toxic signs during this recovery period. While the observed pronounced pulmonary toxicity is arguably linkable to the fact that lung is the AgNPs portal entry, the hepatic response can be ascribable either to NPs

translocation from the lung to the systemic circulation as well as to a secondary organ alteration induced by spreading inflammatory factors released from the lung following sudden local insult [86].

Concerning the toxicity mechanism, literature data suggested that the ionic silver released from the particle surface is the actual species that accounts for the toxicity of AgNPs [87]. Other experimental studies have indeed demonstrated a certain release of ions from the surface of AgNPs [23,51,88] that remained stable over several months. In our study, the concomitant administration of AgNP and AgNO₃ (being the latter frequently used as the precursor of AgNPs during NP chemical synthesis) allowed us to explore their comparative toxic effects on rat lung and liver. We calculated that animals, belonging to different experimental groups, received an equivalent dose of ionic silver, i.e. 7 µg/rat AgNO₃, corresponding to 4.4 µg Ag, or 50 µg/rat AgNPs, corresponding to approximately 6 µg/rat of silver ions (based on the notion that AgNPs used in the present study released 11% of their Ag content as ionic silver). Based on our findings, we cannot exclude that Ag ions released from the instilled AgNPs may have a role in inducing toxicity and tissue damage [85,88], although performed physicochemical characterization (i.e. HRTEM data and Zeta potential value) demonstrated a good stability of the employed AgNPs suspension. Thus, also in accordance to recent *in silico* PBPK data [89], we may hypothesise that the whole, undivided AgNPs are able to trigger the observed adverse

effects.

Since previous experimental findings, applying low AgNPs dose comparable to that used in our investigation, yet demonstrated lung and liver content, with the latter often below the detection limit already 24 h after exposure [61], the kinetics of Ag tissue distribution was not presently examined.

As determined in our previous investigations, the present findings corroborate the occurrence of a NPs diffusive phenomenon, namely *translocation*, demonstrating that AgNPs can cross the alveolar barrier and settle in extrapulmonary organs. In fact, despite the more striking pulmonary effects, distant toxic effects in liver were clearly demonstrated, possibly abetting by the inflammatory status of the lung causing changes in alveolar permeability. The present results integrate our previous findings in kidney [65] revealing AgNPs-caused moderate renal damage in terms of cortical alteration, also involving the vascular component of the renal mesangium. Similarly, these results also matches with our previous data, demonstrating systemic changes in hepatic selected genes of AgNP-treated animals, at early timepoint only [66]. 28th recovery, observed by both genomic and histopathological/ultrastructural analyses, could possibly reflect either compensatory mechanism contrasting the initial toxic response to AgNPs or the silver removal from the tested organs.

Altogether, our results are in accordance with a bulk of recent literature [17,90,91], revealing AgNPs translocation using *in vitro* and *in vivo* approaches, supported by analytical measurements.

In summary, our data demonstrating manifest toxic effects already after a single i.t. exposure to a low AgNPs dose, corroborate the idea that despite the AgNPs widespread use in paint, healthcare and cosmetic applications, several challenges remain to be overcome to fully guarantee the public health safety. Thus, further in depth investigations, based on a multi-tiered approach including an exhaustive physicochemical characterization followed by detailed toxicological studies, would better clarify the AgNPs toxicity mechanisms, improving the overall understanding of the possible adverse outcomes resulting from novel nanotechnology-based products exposure.

Statement on the welfare of animals

All experimental procedures were performed in compliance with the European Council Directive 2010/63/EU on the care and use of laboratory animals. All animals used in this research have been treated humanely according to the institutional guidelines, with due consideration for the alleviation of distress and discomfort.

Funding

This work was supported by the Italian Ministries of Health, Research and Education.

Declaration of Competing Interest

The authors declare no conflict of interest.

Acknowledgments

The authors wish to acknowledge Dr Fabrizio De Luca and Dr Stella Siciliani for their technical support for Light & Electron microscopy imaging, and Professors Aldo Milzani, Isabella Dalle-Donne and Graziano Colombo for the PCO analyses.

References

- [1] H.S. Sharma, S.F. Ali, S.M. Hussain, J.J. Schlager, A. Sharma, Influence of engineered nanoparticles from metals on the blood-brain barrier permeability, cerebral blood flow, brain edema and neurotoxicity. An experimental study in the rat and mice using biochemical and morphological approaches, *J. Nanosci. Nanotechnol.* 9 (2009) 5055–5072.
- [2] E. Iglesias-Silva, J. Rivas, L. Isidro, M. Quintela, Synthesis of silver-coated magnetite nanoparticles, *J. Non-Cryst. Solids* 353 (2007) 829–831, <https://doi.org/10.1016/j.jnoncrysol.2006.12.050>.
- [3] H. Huang, Y. Yang, Preparation of silver nanoparticles in inorganic clay suspensions, *Compos. Sci. Technol.* 68 (2008) 2948–2953, <https://doi.org/10.1016/j.compscitech.2007.10.003>.
- [4] B. Nowack, H.F. Krug, M. Height, 120 years of nanosilver history: implications for policy makers, *Environ. Sci. Technol.* 45 (2011) 1177–1183, <https://doi.org/10.1021/es103316q>.
- [5] E. Hutter, J.H. Fendler, Exploitation of localized surface plasmon resonance, *Adv. Mater.* 16 (2004) 1685–1706, <https://doi.org/10.1002/adma.200400271>.
- [6] S. Sudrik, N. Chaki, V. Chavan, S. Chavan, Silver nanocluster redox-couple-promoted nonclassical electron transfer: an efficient electrochemical Wolff rearrangement of α -diazoketones, *Chemistry* 12 (2006) 859–864.
- [7] Y. Choi, N. Ho, C. Tung, Sensing phosphatase activity by using gold nanoparticles, *Angew. Chem. Int. Engl.* 46 (2007) 707–709, <https://doi.org/10.1002/anie.200603735>.
- [8] K. Yoosaf, B. Ipe, C.H. Suresh, K.G. Thomas, In situ synthesis of metal nanoparticles and selective naked-eye detection of lead ions from aqueous media, *J. Phys. Chem. C* 111 (2007) 12839–12847, <https://doi.org/10.1021/jp073923q>.
- [9] E. Castro-Longoria, A.R. Vilchis-Nestor, M. Avalos-Borja, Biosynthesis of silver, gold and bimetallic nanoparticles using the filamentous fungus *Neurospora crassa*, *Colloids Surf. B Biointerfaces* 83 (2011) 42–48, <https://doi.org/10.1016/j.colsurf.2010.10.035>.
- [10] D. Voelker, K. Schlich, L. Hohndorf, W. Koch, U. Kuehnen, C. Polleichtner, C. Kussatz, K. Hund-Rinke, Approach on environmental risk assessment of nanosilver released from textiles, *Environ. Res.* 140 (2015) 661–667, <https://doi.org/10.1016/j.envres.2015.05.011>.
- [11] N. Gokarneshan, K. Velumani, Application of nano silver particles on textile materials for improvement of antibacterial finishes, *Glob. J. Nanomed.* 2 (2017) 555586, <https://doi.org/10.19080/GJN.2017.02.555586>.
- [12] L. Ge, Q. Li, M. Wang, J. Oujang, X. Li, M.M.Q. Xing, Nanosilver particles in medical applications: synthesis, performance, and toxicity, *Int. J. Nanomedicine* 9 (2014) 2399–2407, <https://doi.org/10.2147/IJN.S55015>.
- [13] P. Hartemann, H. P. A. Proykova, T. Fernandes, A. Baun, W. De Jong, J. Filser, A. Hensten, C. Kneuer, J.-Y. Maillard, H. Norppa, M. Scheringer, S. Wijnhoven, Nanosilver: safety, health and environmental effects and role in antimicrobial resistance, *Mater. Today* 18 (2015) 122–123, <https://doi.org/10.1016/j.mattod.2015.02.014>.
- [14] SCENIHR (Scientific Committee on Emerging and Newly Identified Health Risks), Final Opinion on the Guidance on the Determination of Potential Health Effects of Nanomaterials Used in Medical Devices, January 2015 (2015) https://ec.europa.eu/health/scientific_committees/emerging/docs/scenihr_o_045.pdf.
- [15] E. McGillicuddy, I. Murray, S. Kavanagh, L. Morrison, A. Fogarty, M. Cormican, P. Dockery, M. Prendergast, N. Rowan, D. Morris, Silver nanoparticles in the environment: sources, detection and ecotoxicology, *Sci. Total Environ.* 575 (2017) 231–246, <https://doi.org/10.1016/j.scitotenv.2016.10.041>.
- [16] A. Mackevica, H.S. Foss, Release of nanomaterials from solid nanocomposites and consumer exposure assessment - a forward-looking review, *Nanotoxicology* 10 (2016) 641–653, <https://doi.org/10.3109/17435390.2015.1132346>.
- [17] C. Liao, Y. Li, S.C. Tjong, Bactericidal and cytotoxic properties of silver nanoparticles, *Int. J. Mol. Sci.* 20 (2019) 449, <https://doi.org/10.3390/ijms20020449>.
- [18] K.S. Song, J.H. Sung, J.H. Ji, J.H. Lee, J.S. Lee, H.R. Ryu, J.K. Lee, Y.H. Chung, H.M. Park, B.S. Shin, H.K. Chang, B. Kelman, I.J. Yu, Recovery from silver-nanoparticle-exposure-induced lung inflammation and lung function changes in Sprague Dawley rats, *Nanotoxicology* 7 (2013) 169–180, <https://doi.org/10.3109/17435390.2011.648223>.
- [19] P.P. Simeonova, A. Erdely, Engineered nanoparticle respiratory exposure and potential risks for cardiovascular toxicity: predictive tests and biomarkers, *Inhal. Toxicol.* 21 (2009) 68–73, <https://doi.org/10.1080/08958370902942566>.
- [20] M.S. Heydarnejad, P. Yarmohammadi-Samani, M. Mobini Dehkordi, M. Shadkhast, S. Rahnama, Histopathological effects of nanosilver (Ag-NPs) in liver after dermal exposure during wound healing, *Nanomed. J.* 1 (2014) 191–197.
- [21] S. Gaillet, J.-M. Rouanet, Silver nanoparticles: their potential toxic effects after oral exposure and underlying mechanisms - A review, *Food Chem. Toxicol.* 77 (2015) 58–63, <https://doi.org/10.1016/j.fct.2014.12.019>.
- [22] S.W.P. Wijnhoven, W.J.G.M. Peijnen, C.A. Herberths, W.I. Hagens, A.G. Oomen, E.H.W. Heugens, B. Roszek, J. Bisschops, I. Gossens, D. Van De Meent, S. Dekkers, W.H. De Jong, M. van Zijverden, A.J.A.M. Sips, R.E. Geertsma, Nanosilver: a review of available data and knowledge gaps in human and environmental risk assessment, *Nanotoxicology* 3 (2009) 109–138, <https://doi.org/10.1080/17435390902725914>.
- [23] K. Loeschner, N. Hadrup, K. Qvortrup, A. Larsen, X. Gao, U. Vogel, A. Mortensen, H.R. Lam, E.H. Larsen, Distribution of silver in rats following 28 days of repeated oral exposure to silver nanoparticles or silver acetate, *Part. Fibre Toxicol.* 8 (2011) 18, <https://doi.org/10.1186/1743-8977-8-18>.
- [24] J. Costanza, A.M. El Badawy, T.M. Tolaymat, Comment on "120 Years of nanosilver history: implications for policy makers", *Environ. Sci. Technol.* 45 (2011) 7591–7592, <https://doi.org/10.1021/es200666n>.
- [25] B. Schäfer, J.V. Brocke, A. Epp, M. Götz, F. Herzberg, C. Kneuer, Y. Sommer, J. Tentschert, M. Noll, I. Günther, U. Banasiak, G.F. Böhl, A. Lampen, A. Luch, A. Hensel, State of the art in human risk assessment of silver compounds in consumer products: a conference report on silver and nanosilver held at the BfR in 2012, *Arch. Toxicol.* 87 (2013) 2249–2262, <https://doi.org/10.1007/s00204-013-1083-8>.
- [26] SCENIHR (Scientific Committee on Emerging and Newly Identified Health Risks),

- Nanosilver: Safety, Health and Environmental Effects and Role in Antimicrobial Resistance, June 2014 (2014) https://ec.europa.eu/health/scientific_committees/emerging/docs/scenih_r_039.pdf.
- [27] A. Manke, L. Wang, Y. Rojanasakul, Mechanisms of nanoparticle-induced oxidative stress and toxicity, *Biomed Res. Int.* 2013 (2013) (2013), <https://doi.org/10.1155/2013/942916> ID 942916.
- [28] M.M. Dobrzynska, A. Gajownik, J. Radzikowska, A. Lankoff, M. Dusinska, M. Kruszewski, Genotoxicity of silver and titanium dioxide nanoparticles in bone marrow cells of rats in vivo, *Toxicology* 315 (2014) 86–91, <https://doi.org/10.1016/j.tox.2013.11.012>.
- [29] H.R. Mohamed, Estimation of TiO₂ nanoparticle-induced genotoxicity persistence and possible chronic gastritis-induction in mice, *Food Chem. Toxicol.* 83 (2015) 76–83, <https://doi.org/10.1016/j.fct.2015.05.018>.
- [30] M. Ahamed, R. Posgai, T.J. Gorey, M. Nielsen, S.M. Hussain, J.J. Rowe, Silver nanoparticles induced heat shock protein 70, oxidative stress and apoptosis in *Drosophila melanogaster*, *Toxicol. Appl. Pharmacol.* 242 (2010) 263–269, <https://doi.org/10.1016/j.taap.2009.10.016>.
- [31] H.J. Johnston, G. Hutchison, F.M. Christensen, S. Peters, S. Hankin, V. Stone, A review of the in vivo and in vitro toxicity of silver and gold particulates: particle attributes and biological mechanisms responsible for the observed toxicity, *Crit. Rev. Toxicol.* 40 (2010) 328–346, <https://doi.org/10.3109/10408440903453074>.
- [32] F.M. Christensen, H.J. Johnston, V. Stone, R.J. Aitken, S. Hankin, S. Peters, K. Aschberger, Nano-silver-feasibility and challenges for human health risk assessment based on open literature, *Nanotoxicology* 4 (2010) 284–295, <https://doi.org/10.3109/17435391003690549>.
- [33] S. Jahan, I.B. Yusoff, Y.B. Alias, A.F.B.A. Bakar, Reviews of the toxicity behavior of five potential engineered nanomaterials (ENMs) into the aquatic ecosystem, *Toxicol. Rep.* 4 (2017) 211–220, <https://doi.org/10.1016/j.toxrep.2017.04.001>.
- [34] C. Recordati, M. de Maglie, S. Bianchissi, S. Argenti, C. Cella, S. Mattiello, F. Cubadda, F. Aureli, M. D'Amato, A. Raggi, C. Lenardi, P. Milani, E. Scanziani, Tissue distribution and acute toxicity of silver after single intravenous administration in mice: nano-specific and size-dependent effects, *Part. Fibre Toxicol.* 13 (2016) 12, <https://doi.org/10.1186/s12989-016-0124-x>.
- [35] H.R. Kim, Y.J. Park, D.Y. Shin, S.M. Oh, K.H. Chung, Appropriate in vitro methods for genotoxicity testing of silver nanoparticles, *Environ. Health Toxicol.* 28 (2013), <https://doi.org/10.5620/eht.2013.28.e2013003> ID: e2013003.
- [36] A. Daphedar, T.C. Taranath, Characterization and cytotoxic effect of biogenic silver nanoparticles on mitotic chromosomes of *Drimys polyantha* (Blatt. & McCann) Stearn, *Toxicol. Rep.* 5 (2018) 910–918, <https://doi.org/10.1016/j.toxrep.2018.08.018>.
- [37] D. McShan, P.C. Ray, H. Yu, Molecular toxicity mechanism of nanosilver, *J. Food Drug Anal.* 22 (2014) 116–127, <https://doi.org/10.1016/j.jfda.2014.01.010>.
- [38] A.R. Gliga, S. Skoglund, I.O. Wallinder, B. Fadeel, H.L. Karlsson, Size-dependent cytotoxicity of silver nanoparticles in human lung cells: the role of cellular uptake, agglomeration and Ag release, *Part. Fibre Toxicol.* 11 (2014) 11, <https://doi.org/10.1186/1743-8977-11-11>.
- [39] J.P. Pani, S. Pani, R. Singh, Apoptosis, Necrosis and Cytotoxicity of Newly Emerging and Developing Precursor Hepatoblast and Neuroblast Stem Cells After Critical Cell and Nucleoli Core Penetration of Small Size Nano Silver, *J. Stem Cell. Biol. Blood Marrow Transplant.* 2 (2018) 2, <https://doi.org/10.21767/2575-7725.100019>.
- [40] Y.S. Kim, M.Y. Song, J.D. Park, K.S. Song, H.R. Ryu, Y.H. Chung, et al., Subchronic oral toxicity of silver nanoparticles, *Part. Fibre Toxicol.* 7 (2010) 20, <https://doi.org/10.1186/1743-8977-7-20>.
- [41] M.J. Piao, K.A. Kang, I.K. Lee, H.S. Kim, S. Kim, J.Y. Choi, J. Choi, J.W. Hyun, Silver nanoparticles induce oxidative cell damage in human liver cells through inhibition of reduced glutathione and induction of mitochondria-involved apoptosis, *Toxicol. Lett.* 201 (2011) (2011) 92–100, <https://doi.org/10.1016/j.toxlet.2010.12.010>.
- [42] D. He, A.M. Jones, S. Garg, D.T. Waite, Silver nanoparticle and reactive oxygen species interactions: application of a charging-discharging model, *J. Phys. Chem. C* 115 (2011) 5461–5468, <https://doi.org/10.1021/jp111275a>.
- [43] C. Völker, M. Oetken, J. Oehlmann, The biological effects and possible modes of action of nanosilver, *Rev. Environ. Contam. Toxicol.* 223 (2013) 81–106, https://doi.org/10.1007/978-1-4614-5577-6_4.
- [44] A. Onodera, F. Nishiumi, K. Kakiguchi, A. Tanaka, N. Tanabe, A. Honma, K. Yamaya, Y. Yoshioka, K. Nakahira, S. Yonemura, I. Yanagihara, Y. Tsutsumi, Y. Kawai, Short-term changes in intracellular ROS localisation after the silver nanoparticles exposure depending on particle size, *Toxicol. Rep.* 2 (2015) 574–579, <https://doi.org/10.1016/j.toxrep.2015.03.004>.
- [45] P. Rajanahalli, C.J. Stucke, Y. Hong, The effects of silver nanoparticles on mouse embryonic stem cell self-renewal and proliferation, *Toxicol. Rep.* 2 (2015) 758–764, <https://doi.org/10.1016/j.toxrep.2015.05.005>.
- [46] L. Pauksch, M. Rohnke, R. Schnettler, K.S. Lips, Silver nanoparticles do not alter human osteoclastogenesis but induce cellular uptake, *Toxicol. Rep.* 1 (2014) 900–908, <https://doi.org/10.1016/j.toxrep.2014.10.012>.
- [47] I. Iavicoli, L. Fontana, G. Nordberg, The effects of nanoparticles on the renal system, *Crit. Rev. Toxicol.* 46 (2016) 490–560, <https://doi.org/10.1080/10408444.2016.1181047>.
- [48] L.L. Davenport, H. Hsieh, B.L. Eppert, V.S. Carreira, M. Krishan, T. Ingle, P.C. Howard, M.T. Williams, M.B. Gender, Systemic and behavioral effects of intranasal administration of silver nanoparticles, *Neurotoxicol. Teratol.* 51 (2015) 68–76, <https://doi.org/10.1016/j.ntt.2015.08.006>.
- [49] W.H. De Jong, L.T. van der Ven, A. Sleijffers, M.V. Park, E.H. Jansen, H. van Loveren, R.J. Vandebriel, Systemic and immunotoxicity of silver nanoparticles in an intravenous 28 days repeated dose toxicity study in rats, *Biomaterials* 34 (2013) 8333–8343, <https://doi.org/10.1016/j.biomaterials.2013.06.048>.
- [50] B. Shahare, M. Yashpal, Toxic effects of repeated oral exposure of silver nanoparticles on small intestine mucosa of mice, *Toxicol. Mech. Methods* 23 (2013) 161–167, <https://doi.org/10.3109/15376516.2013.764950>.
- [51] M. Van der Zande, R.J. Vandebriel, E. van Doren, E. Kramer, Z. Herrera Rivera, C.S. Serrano-Rojero, E.R. Gremmer, J. Mast, Peters R.J., P.C. Hollman, P.J.M. Hendriksen, H.J.P. Marvin, A.A.C.M. Peijnenburg, H. Bouwmeester, Distribution, elimination, and toxicity of silver nanoparticles and silver ions in rats after 28-day oral exposure, *ACS Nano* 6 (2012) (2012) 7427–7442, <https://doi.org/10.1021/nn302649p>.
- [52] B.K. Gaiser, T.F. Fernandes, M.A. Jepson, J.R. Lead, C.R. Tyler, M. Baalousha, A. Biswas, G.J. Britton, P.A. Cole, B.D. Johnston, et al., Interspecies comparisons on the uptake and toxicity of silver and cerium dioxide nanoparticles, *Environ. Toxicol. Chem.* 31 (2012) 144–154, <https://doi.org/10.1002/etc.703>.
- [53] S. Kim, D.Y. Ryu, Silver nanoparticle-induced oxidative stress, genotoxicity and apoptosis in cultured cells and animal tissues, *J. Appl. Toxicol.* 33 (2013) 78–89, <https://doi.org/10.1002/jat.2792>.
- [54] J.P. Pani, R. Singh, Small size nanosilver multi organ toxicity: a higher dose negative response in vivo and in vitro experimental application, *Biomed. J. Sci. & Tech. Res.* 1 (4) (2017), <https://doi.org/10.26717/BJSTR.2017.01.000360> (2017b).
- [55] H. Wen, M. Dan, Y. Yang, J. Lyu, A. Shao, X. Cheng, L. Chen, L. Xu, Acute toxicity and genotoxicity of silver nanoparticle in rats, *PLoS One* 12 (2017), <https://doi.org/10.1371/journal.pone.0185554> ID: e0185554.
- [56] E.J. Park, E. Bae, J. Yi, Y. Kim, K. Choi, S.H. Lee, J. Yoon, B.C. Lee, K. Park, Repeated-dose toxicity and inflammatory responses in mice by oral administration of silver nanoparticles, *Environ. Toxicol. Pharmacol.* 30 (2010) 162–168, <https://doi.org/10.1016/j.etap.2010.05.004>.
- [57] S. Takenaka, E. Karg, C. Roth, H. Schulz, A. Ziesenis, U. Heinzmann, P. Schramel, J. Heyder, Pulmonary and systemic distribution of inhaled ultrafine silver particles in rats, *environ. Health Perspect.* 109 (2001) 547–551, <https://doi.org/10.1289/ehp.01109s4547>.
- [58] S. Kitter, C. Greulich, J. Diendorf, M. Koller, M. Epple, Toxicity of silver nanoparticles increases during storage because of slow dissolution under release of silver ions, *Chem. Mater.* 22 (2010) 4548–4554, <https://doi.org/10.1021/cm100023p>.
- [59] K.E. Driscoll, D.L. Costa, G. Hatch, R. Henderson, G. Oberdorster, H. Salem, R.B. Schlesinger, Intratracheal instillation as an exposure technique for the evaluation of respiratory tract toxicity: uses and limitations, *Toxicol. Sci.* 55 (2000) 24–35, <https://doi.org/10.1093/toxsci/55.1.24>.
- [60] D. Elgrabli, S. Abella-Gallart, F. Robidel, F. Rogerieux, J. Boczkowski, G. Lacroix, Induction of apoptosis and absence of inflammation in rat lung after intratracheal instillation of multiwalled carbon nanotubes, *Toxicology* 253 (2008) 131–136, <https://doi.org/10.1016/j.tox.2008.09.004>.
- [61] Y. Arai, T. Miyayama, S. Hirano, Difference in the toxicity mechanism between ion and nanoparticle forms of silver in the mouse lung and in macrophages, *Toxicology* 328 (2015) 84–92, <https://doi.org/10.1016/j.tox.2014.12.014>.
- [62] E.R. Weibel, Stereological methods, *Practical Methods for Biological Morphometry Vol 1* Academic Press Inc, London, 1979, <https://doi.org/10.1002/jobm.19810210824>.
- [63] I. Dalle-Donne, M. Carini, M. Orioli, G. Vistoli, L. Regazzoni, G. Colombo, R. Rossi, A. Milzani, G. Aldini, Protein carbonylation: 2,4-dinitrophenylhydrazine reacts with both aldehydes/ketones and sulfenic acids, *Free Radic. Biol. Med.* 46 (2009) 1411–1419, <https://doi.org/10.1016/j.freeradbiomed.2009.02.024>.
- [64] G. Colombo, M. Clerici, M.E. Garavaglia, D. Giustarini, R. Rossi, A. Milzani, I. Dalle-Donne, A step-by-step protocol for assaying protein carbonylation in biological samples, *J. Chromatogr. B* 1019 (2016) 178–190, <https://doi.org/10.1016/j.jchromb.2015.11.052>.
- [65] E. Roda, S. Barni, A. Milzani, I. Dalle-Donne, G. Colombo, T. Coccini, Single silver nanoparticle instillation induced early and persisting moderate cortical damage in rat kidneys, *Int. J. Mol. Sci.* 18 (2017) 2115, <https://doi.org/10.3390/ijms18102115>.
- [66] T. Coccini, R. Gornati, F. Rossi, E. Signoretto, I. Vanetti, G. Bernardini, L. Manzo, Gene expression changes in rat liver and testes after lung instillation of a low dose of silver nanoparticles, *J. Nanomed. Nanotechnol.* 5 (2014) 5, <https://doi.org/10.4172/2157-7439.1000227>.
- [67] A. Rókus, D. Veres, A. Szűcs, E. Bugyi, M. Mózes, S. Paku, P. Nagy, K. Dezső, Ductular reaction correlates with fibrogenesis but does not contribute to liver regeneration in experimental fibrosis models, *PLoS One* 12 (2017), <https://doi.org/10.1371/journal.pone.0176518> ID: e0176518.
- [68] L. Ulm, A. Krivohlavek, D. Jurašin, M. Ljubojević, G. Šinko, T. Crnković, I. Žuntar, S. Šikić, I. Vinković Vrček, Response of biochemical biomarkers in the aquatic crustacean *Daphnia magna* exposed to silver nanoparticles, *Environ. Sci. Pollut. Res. Int.* 22 (2015) 19990–19999, <https://doi.org/10.1007/s11356-015-5201-4>.
- [69] T.Y. Lee, M.S. Liu, L.J. Huang, S.I. Lue, L.C. Lin, A.L. Kwan, R.C. Yang, Bioenergetic failure correlates with autophagy and apoptosis in rat liver following silver nanoparticle intraperitoneally administration, *Part. Fibre Toxicol.* 10 (2013) 40, <https://doi.org/10.1186/1743-8977-10-40>.
- [70] O.M. Sarhan, H. R.M. Effects of intraperitoneally injected silver nanoparticles on histological structures and blood parameters in the albino rat, *Int. J. Nanomed. Nanosurg.* 9 (2014) 1505–1517, <https://doi.org/10.2147/IJN.S56729>.
- [71] L. Yang, H. Kuang, W. Zhang, Z.P. Aguilar, H. Wei, H. Xu, Comparisons of the biodistribution and toxicological examinations after repeated intravenous administration of silver and gold nanoparticles in mice, *Sci. Rep.* 7 (2017) 3303, <https://doi.org/10.1038/s41598-017-03015-1>.
- [72] D.S. Anderson, R.M. Silva, D. Lee, P.C. Edwards, A. Sharmah, T. Guo, K.E. Pinkerton, L.S. Van Winkle, Persistence of silver nanoparticles in the rat lung: influence of dose, size, and chemical composition, *Nanotoxicology* 9 (2015) 591–602, <https://doi.org/10.3109/17435390.2014.958116>.

- [73] N. Li, S. Georas, N. Alexis, P. Fritz, T. Xia, M.A. Williams, E. Horner, A. Nel, A work group report on ultrafine particles (American Academy of Allergy, Asthma & Immunology): why ambient ultrafine and engineered nanoparticles should receive special attention for possible adverse health outcomes in human subjects, *J. Allergy Clin. Immunol.* 138 (2016) 386–396, <https://doi.org/10.1016/j.jaci.2016.02.023>.
- [74] Y. Morimoto, H. Izumi, Y. Yoshiura, K. Fujishima, K. Yatera, K. Yamamoto, Usefulness of intratracheal instillation studies for estimating nanoparticle-induced pulmonary toxicity, *Int. J. Mol. Sci.* 17 (2016) 165, <https://doi.org/10.3390/ijms17020165>.
- [75] R.M. Silva, D.S. Anderson, L.M. Franzi, J.L. Peake, P.C. Edwards, L.S. van Winkle, K.E. Pinkerton, Pulmonary effects of silver nanoparticle size, coating, and dose over time upon intratracheal instillation, *Toxicol. Sci.* 144 (2015) 151–162, <https://doi.org/10.1093/toxsci/kfu265>.
- [76] S. Smulders, K. Luyts, G. Brabants, K. van Landuyt, C. Kirschhock, E. Smolders, L. Golanski, J. Vanoirbeek, P.H.M. Hoet, Toxicity of nanoparticles embedded in paints compared with pristine nanoparticles in mice, *Toxicol. Sci.* 141 (2014) 132–140, <https://doi.org/10.1093/toxsci/kfu112>.
- [77] E. Sadauskas, H. Wallin, M. Stoltenberg, U. Vogel, P. Doering, A. Larsen, G. Danscher, Kupffer cells are central in the removal of nanoparticles from the organism, *Part. Fibre Toxicol.* 4 (2007) 10, <https://doi.org/10.1186/1743-8977-4-10>.
- [78] K. Dziendzikowska, J. Gromadzka-Ostrowska, A. Lankoff, M. Oczkowska, A. Krawczynska, J. Chwastowska, M. Sadowska-Bratek, E. Chajduk, M. Wojewodzka, M. Kruszewski, Time-dependent biodistribution and excretion of silver nanoparticles in male Wistar rats, *J. Appl. Toxicol.* 32 (2012) 920–928, <https://doi.org/10.1002/jat.2758>.
- [79] G. Qin, S. Tang, S. Li, H. Lu, Y. Wang, P. Zhao, B. Li, J. Zhang, L. Peng, Toxicological evaluation of silver nanoparticles and silver nitrate in rats following 28 days of repeated oral exposure, *Environ. Toxicol.* 32 (2017) 609–618, <https://doi.org/10.1002/tox.22263>.
- [80] A. Singh, M.Y. Dar, B. Joshi, B. Sharma, S. Shrivastava, S. Shukla, Phytofabrication of Silver nanoparticles: novel drug to overcome hepatocellular ailments, *Toxicol. Rep.* 5 (2018) 333–342, <https://doi.org/10.1016/j.toxrep.2018.02.013>.
- [81] M.P. Sutunkova, L.I. Privalova, I.A. Minigalieva, V.B. Gurvich, V.G. Panov, B.A. Katsnelson, The most important inferences from the Ekaterinburg nanotoxicology team's animal experiments assessing adverse health effects of metallic and metal oxide nanoparticles, *Toxicol. Rep.* 5 (2018) 363–376, <https://doi.org/10.1016/j.toxrep.2018.03.008>.
- [82] A.A. Keller, S. McFerran, A. Lazareva, S. Suh, Global life cycle releases of engineered nanomaterials, *J. Nanopart. Res.* 15 (2013) 1692, <https://doi.org/10.1007/s11051-013-1692-4>.
- [83] G. Oberdörster, E. Oberdörster, J. Oberdörster, Nanotoxicology: an emerging discipline evolving from studies of ultrafine particles, *Environ. Health Perspect.* 113 (2005) 823–839, <https://doi.org/10.1289/ehp.7339>.
- [84] L. Garza-Ocanas, D.A. Ferrer, J. Burt, L.A. Diaz-Torres, M. Ramírez Cabrera, V.T. Rodríguez, R. Luján Rangel, D. Romanovicz, M. Jose-Yacaman, Biodistribution and long-term fate of silver nanoparticles functionalized with bovine serum albumin in rats, *Met. Integr. Biometal. Sci.* 2 (2010) 204–210, <https://doi.org/10.1039/b916107d>.
- [85] S. Juling, G. Bachler, N. von Goetz, D. Lichtenstein, L. Böhmert, A. Niedzwiecka, S. Selve, A. Braeuning, A. Lampen, In vivo distribution of nanosilver in the rat: the role of ions and *de novo*-formed secondary particles, *Food Chem. Toxicol.* 97 (2016) 327–335, <https://doi.org/10.1016/j.fct.2016.08.016>.
- [86] T. Coccini, S. Barni, L. Manzo, E. Roda, Apoptosis induction and histological changes in rat kidney following Cd-doped silica nanoparticle exposure: evidence of persisting effects, *Toxicol. Mech. Methods* 23 (2013) 566–575, <https://doi.org/10.3109/15376516.2013.803270>.
- [87] H. Bouwmeester, J. Poortman, R.J. Peters, E. Wijma, E. Kramer, et al., Characterization of translocation of silver nanoparticles and effects on whole-genome gene expression using an in vitro intestinal epithelium co-culture model, *ACS Nano* 5 (2011) 4091–4103.
- [88] J.L. Falconer, J.A. Alt, D.W. Grainger, Comparing ex vivo and in vitro translocation of silver nanoparticles and ions through human nasal epithelium, *Biomaterials* 171 (2018) 97–106, <https://doi.org/10.1016/j.biomaterials.2018.04.013>.
- [89] G. Bachler, N. von Goetz, K. Hungerbühler, A physiologically based pharmacokinetic model for ionic silver and silver nanoparticles, *Int. J. Nanomed. Nanosurg.* 8 (2013) 3365–3382, <https://doi.org/10.2147/IJN.S46624>.
- [90] J. Vidmar, K. Loeschner, M. Correia, E.H. Larsen, P. Manser, A. Wichser, K. Boodhia, Z.S. Al-Ahmady, J. Ruiz, D. Astruc, T. Buerki-Thurnherr, Translocation of silver nanoparticles in the ex vivo human placenta perfusion model characterized by single particle ICP-MS, *Nanoscale* 10 (2018) 11980–11991, <https://doi.org/10.1039/C8NR02096E>.
- [91] F. Zhang, G.V. Aquino, A. Dabi, E.D. Bruce, Assessing the translocation of silver nanoparticles using an in vitro co-culture model of human airway barrier, *Toxicol. In Vitro* 56 (2019) 1–9, <https://doi.org/10.1016/j.tiv.2018.12.013>.